Effect of Thermal History on the Time Evolution of the Structure of a Main-Chain Thermotropic Liquid-Crystalline Polyester

Chang Dae Han,* Sukky Chang, and Seung Su Kim†

Department of Polymer Engineering, The University of Akron, Akron, Ohio 44325-0301

Received June 20, 1994; Revised Manuscript Received September 9, 1994®

ABSTRACT: The effect of thermal history on the time evolution of the structure of a main-chain thermotropic liquid-crystalline polymer, poly[(phenylsulfonyl)-*p*-phenylene 1,10-decamethylenebis(4-oxybenzoate)] (PSHQ10), was investigated using differential scanning calorimetry (DSC), wide-angle X-ray diffraction (WAXD), and optical microscopy. For the study, the specimens having the following thermal histories were employed: (a) fully oriented melt-spun fiber, (b) as-cast specimen, and (c) as-cast specimen followed by thermal treatment at 190 °C in the isotropic region. We found that when an as-cast specimen was annealed at 130 °C, it exhibited an *intermediate* endothermic peak at a temperature (T_{m1}) between the crystal melting temperature (T_{m2}) (~120 °C) and the nematic–isotropic transition temperature (T_{NI}) (~180 °C) very soon after the annealing began, but when an as-cast specimen was first heated to 190 °C in the isotropic region followed by annealing at 130 °C, *only* T_{m2} and T_{NI} appeared until the annealing continued for ~40 h and then T_{m1} appeared as the annealing continued further. We found, however, that a melt-spun fiber exhibited *only* T_{m2} and T_{NI} until the annealing continued for ~ 40 h and then T_{m1} appeared as the annealing continued further. By conducting variable heating rate DSC we have concluded that the appearance of T_{m1}, which represents high-temperature melting crystals, originated from the *recrystallization* and *perfection* of the crystals during isothermal annealing. Using WAXD at room temperature and also at elevated temperatures, we confirmed the existence of two forms of crystals in an annealed specimen. During isothermal annealing of the specimens, which had different thermal histories, on a hot-stage microscope under cross-polarized light at 130 °C (which was slightly above T_{m2}), we made the following observations. (a) When using a fully oriented melt-spun fiber, we observed the appearance of *banded structure* initially and then the formation of high-temperature melting crystals, which made the banded structure disappear as the annealing continued for over ~40 h. (b) When using either a melt-spun fiber or an as-cast specimen, which received thermal treatment at 190 °C in the isotropic region, we observed Schlieren textures initially and then the formation of high-temperature melting crystals as the annealing continued for over ~40 h. (c) However, when using an as-cast specimen without thermal treatment, we could not observe distinct Schlieren textures because high-temperature melting crystals were formed immediately after the annealing began.

1. Background

In recent years, using differential scanning calorimetry (DSC), a number of researchers[1–10] observed that some thermotropic liquid-crystalline polymers (TLCPs) exhibit *dual* endothermic peaks at temperatures below their isotropization (or clearing) temperature. Butzbach et al.[3] labeled one endothermic peak, which corresponds to the melting point T_{m2} of the crystalline phase, as a *fast* transition process, and the other endothermic peak, which corresponds to the melting point T_{m1} of the crystals that were formed during annealing, as a *slow* transition process. According to the literature, the value of T_{m1} can be *lower*[1–7] or *higher*[8,9] than that of T_{m2}. The seemingly complicated dual endothermic transition behavior in TLCP observed by various research groups may be summarized as follows.

By annealing the copolyester of 30 mol % *p*-hydroxybenzoic acid (HBA) and 70 mol % poly(ethylene terephthalate) (PET) at temperatures between 135 and 200 °C, Krigbaum and Salaris[1] observed (i) a lower temperature endothermic peak (corresponding to T_{m1}) only in the *annealed* samples, its position and area varying with annealing time, and (ii) a higher temperature endothermic peak (corresponding to T_{m2}) in all samples including one that had *not* been annealed, the area under the peak decreasing with annealing time, but its position remaining more or less *constant* except for one that had been annealed at 200 °C. They concluded that there exist two interconvertible forms of crystals, which differ from each other only in degree of crystal size and perfection, similar to ones observed earlier in neat PET.[11] On the basis of the DSC thermograms obtained for three series of homopolyesters having the repeat unit structure

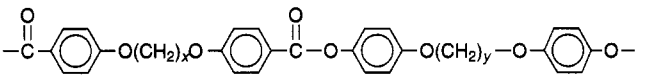

x = 2–10, 12; y = 6, 8, 10

Griffin and Haven[2] reached *virtually* the same conclusion on the origin of dual endothermic peaks that Krigbaum and Salaris[1] had reached earlier.

Using the copolyester of 58 mol % HBA and 42 mol % 6-hydroxy-2-naphtoic acid (HNA), Butzbach et al.[3] observed that, at low annealing temperatures, the value of T_{m1} was lower than that of T_{m2}, but the value of T_{m1} increased rapidly with increasing annealing temperature and eventually exceeded the value of T_{m2}, yielding a crossover. Later, using the 73/27 HBA/HNA copolyester, Lin and Winter[8] reported that the value of T_{m1} was higher than that of T_{m2} when the copolyester had been annealed at temperatures above T_{m2}. On the basis of the results of wide-angle X-ray diffraction (WAXD), Butzbach et al.[3] noted that the intensity of the reflections along the equator increased, relative to the

† Present address: Research and Development Center, Miwon Petrochemical Corp., Ulsan 780-140, Republic of Korea.

® Abstract published in *Advance ACS Abstracts,* November 1, 1994.

0024-9297/94/2227-7699$04.50/0

background, as the annealing time increased and consequently concluded that annealing improved the ordered structure in terms of both the degree of crystallization and increasing registry of the chain molecules. Using 75/25, 58/42, and 30/70 HBA/HNA copolyesters, Cheng[4,5] also made observations which are essentially the same as those made earlier by Butzbach et al.[3] It should be mentioned that, in the studies referred to above, the value of T_{m2} was found to be independent of the annealing temperature and annealing time.

Using a copolyester consisting of *p*-benzenedicarboxylic acid, phenylhydroquinone, and (1-phenylethyl)-hydroquinone, Cheng et al.[6] observed dual endothermic peaks, having a value of T_{m1} lower than that of T_{m2} but with the value of T_{m1} increasing rapidly, while the value of T_{m2} remained more or less constant, as the annealing temperature increased. On the basis of WAXD results, they concluded that the dual transition processes observed for the copolyester did *not* correspond to two different crystal packings as in the cases of HBA/PET and HBA/HNA copolyesters mentioned above, but instead, the crystals grown in these two processes were both monoclinic; i.e., a solid–solid (from monoclinic I to monoclinic II form) transformation took place during the *slow* transition process.

Using a copolyester consisting of Bisphenol E diacetate, isophthalic acid, and 2,6-naphthalenedicarboxylic acid, Nam et al.[7] observed dual endothermic peaks; namely, as the annealing temperature or the annealing time increased, the lower temperature endothermic peak which corresponds to T_{m1} increased, merging into the higher temperature endothermic peak which corresponds to T_{m2}. They attributed the existence of dual endothermic peaks to a melting–recrystallization phenomenon, but did not ascertain whether the two crystals has identical or different structures.

Using an aromatic thermotropic homopolyester, poly[(phenylsulfonyl)-*p*-phenylene 1,10-decamethylenebis(4-oxybenzoate)] (PSHQ10) with the repeat unit structure

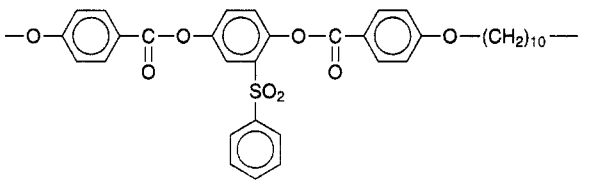

PSHQ10

Kim and Han[9] observed (a) dual endothermic peaks, having a value of T_{m1} higher than that of T_{m2}, and (b) an increase in the rheological properties of PSHQ10 during isothermal annealing at temperatures below its nematic–isotropic transition temperature (T_{NI}), ~175 °C. While speculating that the observed increase in the rheological properties of PSHQ10 was attributable to a continuous change in the *crystallike phase* formed during the isothermal annealing, Kim and Han did not elaborate on the origin(s) of the crystallike phase. Very recently, we conducted an investigation on determining the origin(s) of the crystallike phase in PSHQ10, using DSC, WAXD, and cross-polarized optical microscopy on both solvent-cast films and melt-spun fibers. The purpose of this paper is to present the highlights of our findings, elucidating the structure of the crystallike phase.

The organization of this paper is as follows. First, the experimental results of DSC will be presented, putting emphasis on the effects of (a) thermal history (i.e., annealing temperature and the duration of annealing) of specimens and (b) the method of specimen preparation (i.e., solvent casting versus melt spinning) on dual endothermic transition behavior. Next, the results of WAXD will be presented, putting emphasis on the differences in the WAXD patterns observed between as-cast films and melt-spun fibers. In doing so, we shall present the structures of the crystals, one corresponding to the higher temperature endothermic peak and the other corresponding to the lower temperature endothermic peak. Finally, we shall present cross-polarized optical micrographs taken of the melt-spun fiber speciemens that were subjected to the same thermal histories as those employed for the WAXD experiments.

2. Experimental Section

2.1. Materials. The polymer employed in this study was poly[(phenylsulfonyl)-*p*-phenylene 1,10-decamethylenebis(4-oxybenzoate)] (PSHQ10), which was synthesized, via solution polymerization, in our laboratory. The details of the method of synthesis are given elsewhere.[12,13] The PSHQ10 employed in this study was found via gel permeation chromatography to have a weight-average molecular weight of 48 000 relative to polystyrene standards and a polydispersity of ~2 after several fractionations. The chemical structure of PSHQ10 was confirmed via two-dimensional high-resolution nuclear magnetic resonance spectroscopy.[13]

2.2. Sample Preparation. Specimens for DSC measurements were prepared by (a) solvent casting by dissolving PSHQ10 in dichloromethane in the presence of an antioxidant (Irganox 1010, Ciba-Geigy Group) and then slowly evaporating the solvent at room temperature for 1 week and (b) melt spinning. The as-cast films of 1 mm thickness were further dried at 80 °C for 1 week and then at 120 °C for 2 h in a vacuum oven to remove any residual solvent. Also, thin films of ~1 mm thickness were also prepared by compression molding at 200 °C for 3 min and subsequently cooled slowly to room temperature. The dried PSHQ10 was melt-spun under an isothermal condition (160 °C) using an Instron capillary rheometer, for which a die having the diameter of 1 mm and the length of 8 mm was used. The melt-spinning condition was chosen such that the shear rate inside the die was 20.8 s^{-1} and the takeup ratio (the ratio of the takeup speed and the average velocity at the die exit) was 80. Melt-spun fibers were cooled in ambient air and wound on a takeup roll.

2.3. Differential Scanning Calorimetry. Thermal transition temperatures of the solvent-cast films and melt-spun fibers of PSHQ10 were determined by differential scanning calorimetry (DSC) (du Pont 9900). All DSC runs were made under a nitrogen atmosphere with heating and/or cooling rates of 20 °C/min, and the thermal histories (namely, annealing temperature and the duration of annealing) of the specimens were varied.

2.4. Wide-Angle X-ray Diffraction (WAXD). WAXD experiments were conducted at two different laboratories. High-temperature WAXD experiments were performed on as-cast films by Professor Benjamin Chu and Dr. Y. Li at the Department of Chemistry, State University of New York at Stony Brook, using a Enraf-Nonium rotating-anode X-ray generator operating at 40 kV and 80 mA (Cu Kα radiation, filtered by a Ni foil), Charles Supper double-mirror focusing optics, and an area detector based on a charge-coupled device (CCD) unit. In the experiments, the camera has a sample-to-detector distance of 79 mm and the exposure time for each measurement was 1 h. For the measurements, as-cast films, which had been annealed at 130 °C, were used for variable-temperature WAXD at 23, 130, 165, and 190 °C for a heating cycle and at 190, 165, and 23 °C for a cooling cycle. All the high-temperature WAXD patterns were corrected for detector dark counts and air background. Room-temperature WAXD experiments were performed on both melt-spun fibers and as-cast films at the University of Akron, using a General Electric

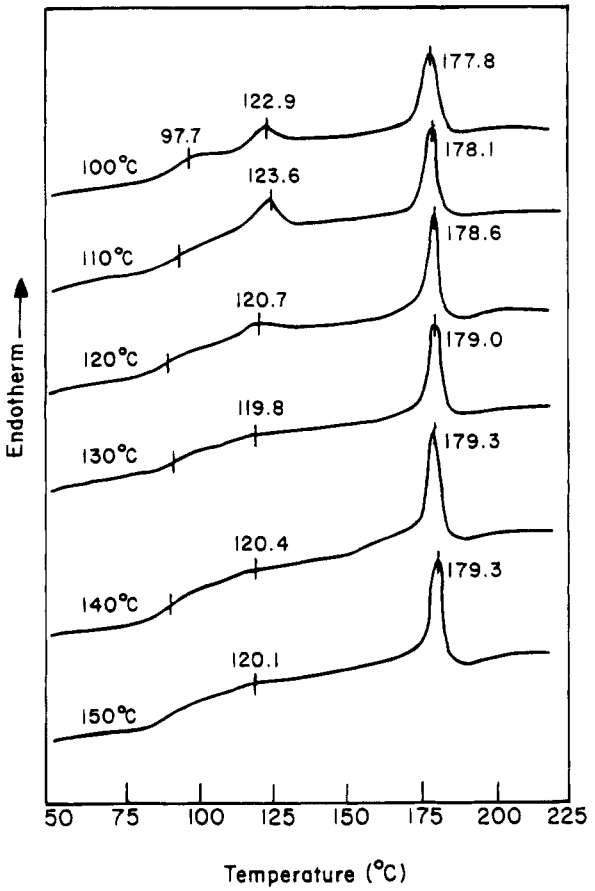

Figure 1. DSC traces for melt-spun PSHQ10 fibers which were annealed for 4 h at various temperatures, as indicated on the plot. The heating rate used was 20 °C/min.

X-ray generator (Model XRD-6) operating at 30 kV and 30 mA (Cu Kα radiation, filtered by a Ni foil). The diffraction patterns were recorded with a camera, which was placed at a distance of 53.3 mm from the specimen. The exposure time for each measurement was 4 h.

2.5. Optical Microscopy. A hot-stage (TH-600 type, Linkham Scientific Co.), microscope (Nikon, Model Optiphoto polXTP-11), with a camera and a programmable temperature controller, and photomicrographic attachment was used to take pictures, under cross-polarized light, of melt-spun fibers which were placed between two slide glasses.

3. Results

3.1. Effect of Thermal History on DSC Thermograms of PSHQ10. Figure 1 gives traces of DSC thermograms of melt-spun fibers, which were annealed for 4 h at various temperatures ranging from 100 to 150 °C. It should be mentioned that a fresh sample was used for each DSC run. It can be seen in Figure 1 that two endothermic peaks appear, one at ~120 °C representing the melting point (T_{m2}) of the crystal (hereafter referred to as *low-temperature melting crystal*) and the other at ~180 °C representing the nematic–isotropic transition temperature (T_{NI}). Note in Figure 1 that the values of both T_{m2} and T_{NI} remain constant, regardless of the annealing temperature employed. However, as the melt-spun fiber was annealed at 130 °C for a longer period, say exceeding 24 h, the traces of DSC thermograms in Figure 2 show that an *intermediate* endothermic peak appears at a temperature (T_{m1}) of ~150 °C but the endothermic peak representing T_{m2} is suppressed. Figure 2 suggests that a crystallike phase (hereafter referred to as *high-temperature melting crystal*) which melts at ~150 °C was formed as a melt-spun fiber was annealed at 130 °C for over 24 h.

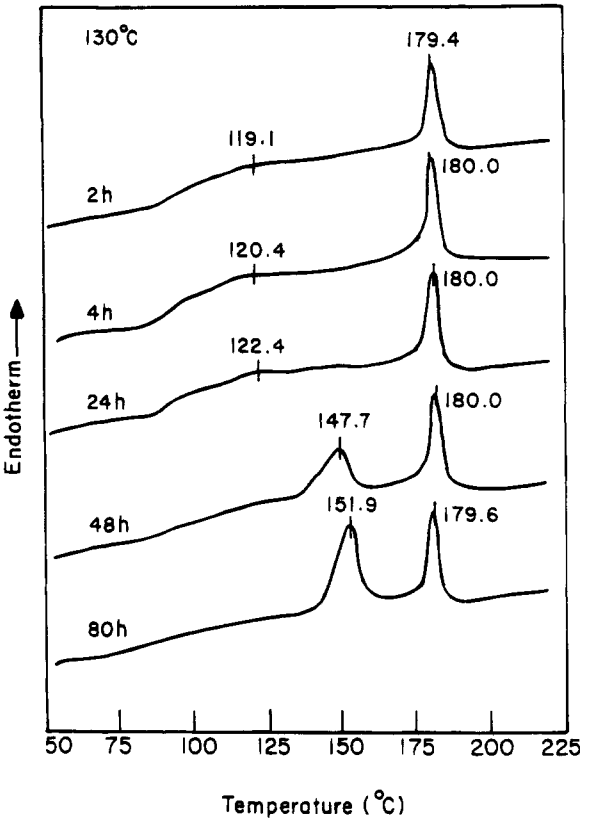

Figure 2. DSC traces for melt-spun PSHQ10 fibers which were annealed at 130 °C for different periods, as indicated on the plot. A fresh specimen was used for each run and the heating rate used was 20 °C/min.

Figure 3 gives traces of DSC thermograms of as-cast specimens, which were annealed at 130 °C for various annealing periods. The following observations are worth making in Figure 3: (a) an *intermediate* endothermic peak representing high-temperature melting crystals appears at 132 °C after annealing for 10 min and this temperature increases to ~150 °C after annealing for 24 h; (b) the peak position (T_{m1}) and the area under the intermediate endothermic peak remain *virtually* constant after the specimen was annealed for 24 h and longer. This seems to indicate that high-temperature melting crystals which were formed during the isothermal annealing at 130 °C attained a *maximum* heat of transition after a specimen was annealed for 24 h.

Figure 4 gives traces of DSC thermograms of an as-cast specimen, which was first thermally treated at 190 °C and then cooled slowly to 130 °C followed by isothermal annealing there. We make the following observations from Figure 4: (a) after being annealed for 20 h, the specimen exhibits two endothermic peaks, one at 127 °C representing the T_{m2} and the other at ~183 °C representing the T_{NI}; (b) after being annealed for 44 h, the specimen exhibits a very mild, additional endothermic peak (T_{m1}) at 150 °C between T_{m2} and T_{NI}, indicating that high-temperature melting crystals were formed during the annealing for a period between 20 and 44 h; (c) when the specimen was annealed for 80 h, the value of T_{m1} increased slightly (to 154 °C); (d) when the specimen was annealed further for 120 h and longer, the value of T_{m1} and the area under the intermediate endothermic peak remain virtually constant; (e) the value of T_{NI} remains constant at ~180 °C, independent

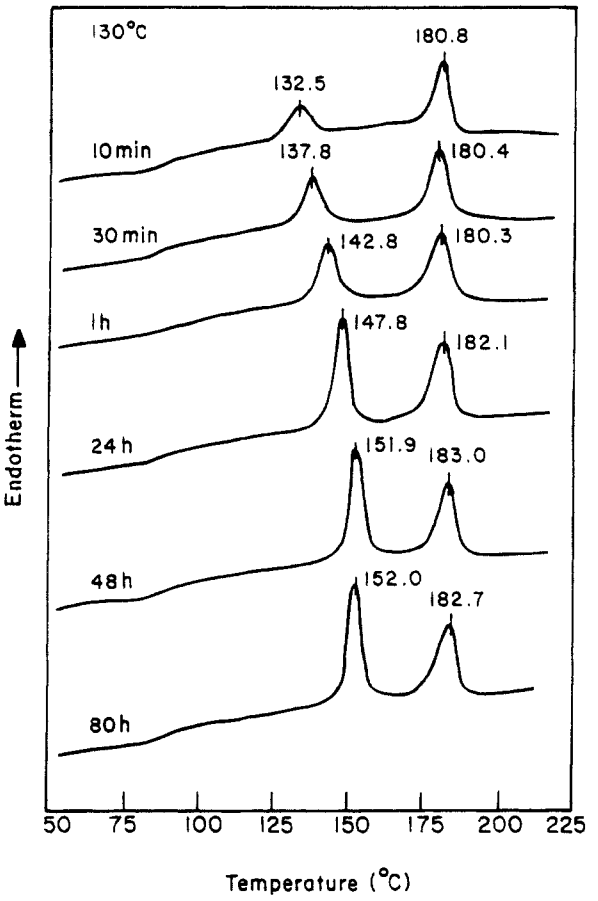

Figure 3. DSC traces for as-cast PSHQ10 specimens which were annealed at 130 °C for different periods, as indicated on the plot. A fresh specimen was used for each run and the heating rate used was 20 °C/min.

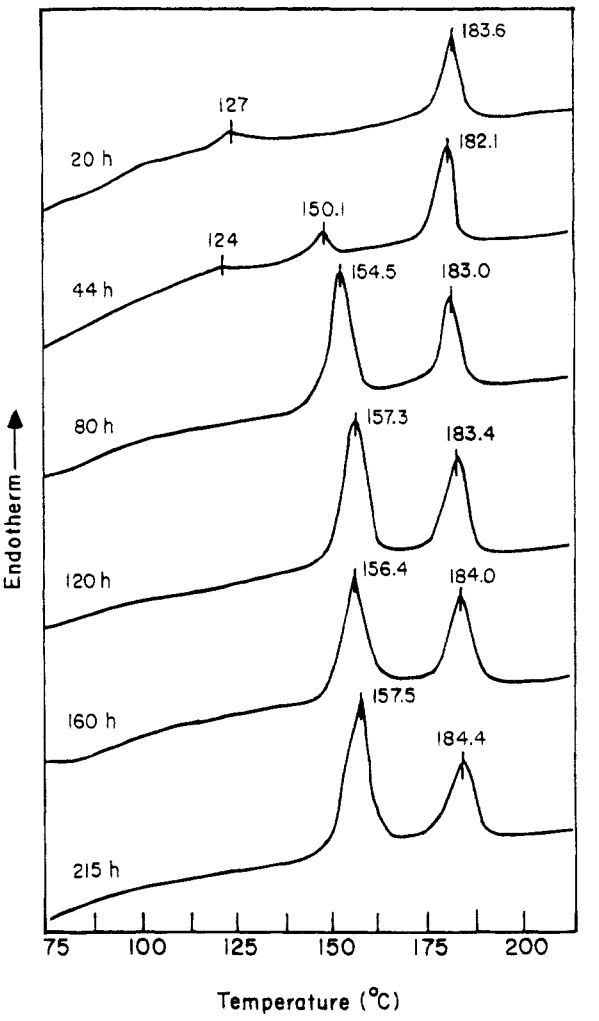

Figure 4. DSC traces for as-cast PSHQ10 specimens which were first heated to 190 °C for 5 min and subsequently annealed at 130 °C for different periods, as indicated on the plot. The heating rate used was 20 °C/min.

of the duration of annealing. The above observations indicate that the formation of high-temperature melting crystals in PSHQ10 is simply delayed if an as-cast specimen was first heated to temperatures in the *isotropic* region followed by slow cooling to the *nematic* region, as compared to the situation where an as-cast specimen was annealed in the nematic region from the beginning. This can be explained as follows: when an as-cast specimen was first heated to the isotropic region, all the domain textures that has existed previously were destroyed, and subsequently, when the specimen was cooled slowly to the nematic region from the isotropic region, a long induction time would be required for the formation of high-temperature melting crystals in PSHQ10.

At this juncture, it is appropriate to mention a study of Bhowmik et al.,[10] who reported that a thermotropic polyester with the repeat unit structure

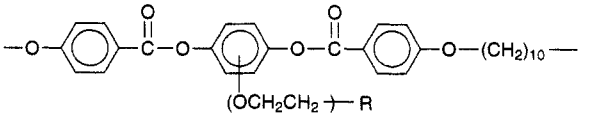

where R is CH_3 or C_2H_5 exhibits two endothermic peaks at temperatures below its T_{NI} and that they reappear during the *repeated* heating and cooling cycles, behavior quite different from that observed in this study. According to Bhowmik et al., an intermediate *endothermic* peak on the DSC thermograms during the *heating cycle* represents the smectic–nematic transition (T_{SN}) and an intermediate *exothermic* peak on the DSC thermograms during the *cooling cycle* represents the nematic–smectic transition (T_{NS}). Thus we conclude that the physical origin for the existence of an *intermediate* endothermic peak observed in Bhowmik's polyester is quite different from that observed in this study, because PSHQ10 does *not* have smectic texture in the anisotropic state.

3.2. WAXD Patterns Taken at Various Temperatures of As-Cast PSHQ10 Specimens Having High-Temperature Melting Crystals. Figure 5 summarizes the variable-temperature WAXD results obtained for an as-cast specimen, which was annealed at 130 °C for 4 h, by first heating from 23 to 190 °C and then cooling from 190 to 23 °C. The following observations are worth noting in Figure 5. (1) Two diffraction peaks corresponding to d = 5.1 and 15.5 Å are observed at both 23 and 130 °C. (2) When the temperature was increased to 165 °C, these two peaks disappeared. We can now conclude that the existence of these two WAXD peaks explains why an intermediate endothermic peak (at 130–160 °C) appeared on the DSC thermograms given in Figures 2–4. (3) Once the two WAXD peaks disappeared as the temperature was increased from 130 to 165 °C, further thermal treatment could not regenerate them. (4) No corresponding WAXD pattern changes are observed when the specimen was further heated from 165 to 190 °C. This probably means that an intermediate endothermic peak that appears at 130–160 °C on the DSC thermograms is involved with a well-ordered crystalline structure. (5) When the specimen

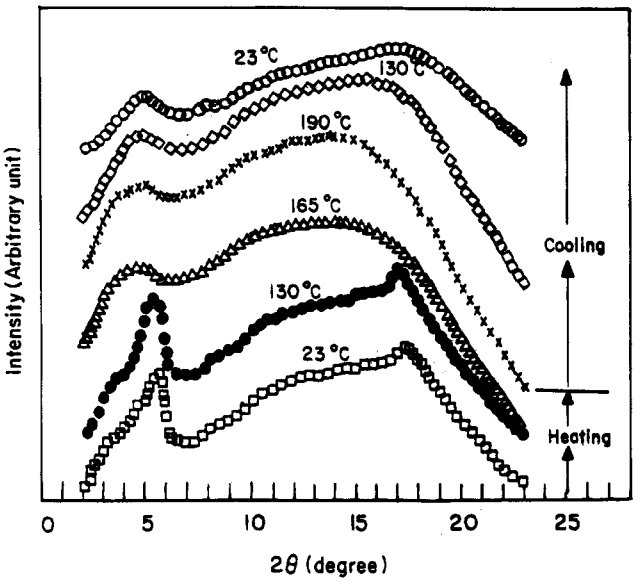

Figure 5. Variation of the X-ray diffraction intensity with scattering angle θ for an as-cast PSHQ10 specimen, which was annealed at 130 °C for 4 h, during the heating and cooling cycles at various temperatures, as indicated on the plot. Two diffraction peaks corresponding to the d-spacings of 5.1 and 15.5 Å, respectively, are seen at both 23 and 130 °C during the heating cycle. However, when the temperature is increased to 165 °C and higher, and also when the temperature is decreased from 190 °C (in the isotropic region) to room temperature, these two diffraction peaks are not seen. Thus, the appearance of these two WAXD peaks is believed to confirm the presence of high-temperature melting crystals which melt away at ~150 °C.

was cooled from 190 to 135 °C, *no* significant WAXD pattern changes were observed, whereas the DSC thermogram during the cooling cycle shows an exothermic peak. This suggests that the *exothermic* peak during the cooling cycle corresponds to the *endothermic* peak at ~180 °C during the heating cycle, and has nothing to do with the endothermic peak at ~150 °C. Again, the isotropic–nematic transition is not involved with any significant changes of well-ordered crystalline structure. (6) No significant WAXD pattern changes may be observed after the PSHQ10 specimen was further cooled to 23 °C.

3.3. Effect of Thermal History on the WAXD Patterns Taken at Room Temperature of Melt-Spun PSHQ10 Fibers. In order to determine the structure of the high-temperature melting crystals in PSHQ10, WAXD patterns were taken at room temperature of melt-spun fibers *with* and *without* annealing. Figure 6 gives WAXD patterns taken of melt-spun fibers having the following thermal histories: (a) without annealing; (b) annealed at 130 °C for 1 h followed by a rapid quenching to room temperature; (c) annealed at 130 °C for 80 h followed by a rapid quenching to room temperature; (d) annealed at 130 °C for 80 h followed by further annealing at 160 °C for 10 min and then rapid quenching to room temperature. The following observations are worth noting in Figure 6. In the melt-spun fiber *without* annealing (see Figure 6a), (a) the equatorial diffraction pattern shows the characteristics typical of liquid-crystalline lateral packing (0.3–0.6 nm); (b) the periodicity of highly aligned fibers is found to be 2.89 nm from the first layer line, which is a symmetric four-point diffraction pattern along the fiber axis; (c) the four-point diffraction spots are elongated horizontally and are perpendicular to the fiber axis, indicating that the reflection planes are inclined from the chain axis (~63°) and the d-spacing of the reflection plane is about 1.35 nm; (d) the four-point reflection pattern is controlled by the width of the chain molecules and the relative longitudinal displacement of neighbors; (e) in addition to the four-point diffraction pattern, which represents the vertical chain periodicity and inclined reflection plane, the meridional reflection over the second layer line shows the d-spacings of 0.976 and 0.494 nm, which correspond to one-third and one-sixth, respectively, of the vertical chain periodicity.

From the X-ray diffraction pattern of the melt-spun fiber that was annealed at 130 °C for 1 h (see Figure 6b), we observe that the chains in the fiber are oriented with angles ranging from 0 to 13° about the fiber axis, and liquid-crystalline lateral spacing is diffused. This is believed to be due to the formation of a *banded structure* on the oriented fibers, evidence of which obtained by optical microscopy under cross-polarized light will be presented later in this paper. However, from the X-ray diffraction pattern of the melt-spun fiber that was annealed for 80 h (see Figure 6c), we make the following observations. (a) The X-ray diffraction pattern shows that along the fiber axis there is some orientation, but to a lesser degree than the fiber that was annealed for *only* 1 h (see Figure 6b). This seems to indicate that owing to the formation of high-temperature melting crystals in the oriented fiber that was annealed for 80 h, some relaxation took place during extended isothermal annealing. (b) The X-ray diffraction pattern in the diffuse liquid-crystalline phase has some specific range (0.3–0.6 nm), and a highly ordered structure can be identified from the equatorial peaks inside the diffuse diffraction patterns having d-spacings of 0.40 and 0.45 nm, indicating that a transformation from a liquid-crystalline structure to an ordered crystallike structure took place during the isothermal annealing for 80 h.

It can be seen in Figure 6d that when a melt-spun fiber, after being annealed at 130 °C for 80 h, was annealed further at 165 °C for 10 min, the two strong diffraction peaks, which represent an ordered crystallike structure (see Figure 6c), disappear and the X-ray diffraction pattern has only diffuse liquid-crystalline structure. It should be remembered that high-temperature melting crystals melt away at ~150 °C (see Figure 2). The partial loss of the fiber orientation along the chain axis observed in Figure 6d is believed to be due to the relaxation of the chains during an extended isothermal annealing. This observation supports our assertion, made above when we presented the results of DSC, that high-temperature melting crystals that melt at ~150 °C were formed when a melt-spun fiber was annealed at 130 °C for a period over 40 h. The values of d-spacing determined for the melt-spun fibers without annealing are given in Table 1, and the values of d-spacing determined for the melt-spun fibers with annealing are given in Table 2.

3.4. Effect of Thermal History on the WAXD Patterns Taken at Room Temperature of As-Cast PSHQ10 Specimens. Figure 7 gives WAXD patterns taken of as-cast specimens having the following thermal histories: (a) without annealing; (b) annealed at 130 °C for 80 h followed by a rapid quenching to room temperature; (c) thermally treated at 190 °C for 10 min followed by a rapid quenching to room temperature; (d) thermally treated at 190 °C for 10 min followed by annealing at 130 °C for 80 h and then rapid quenching to room temperature. The following observations are

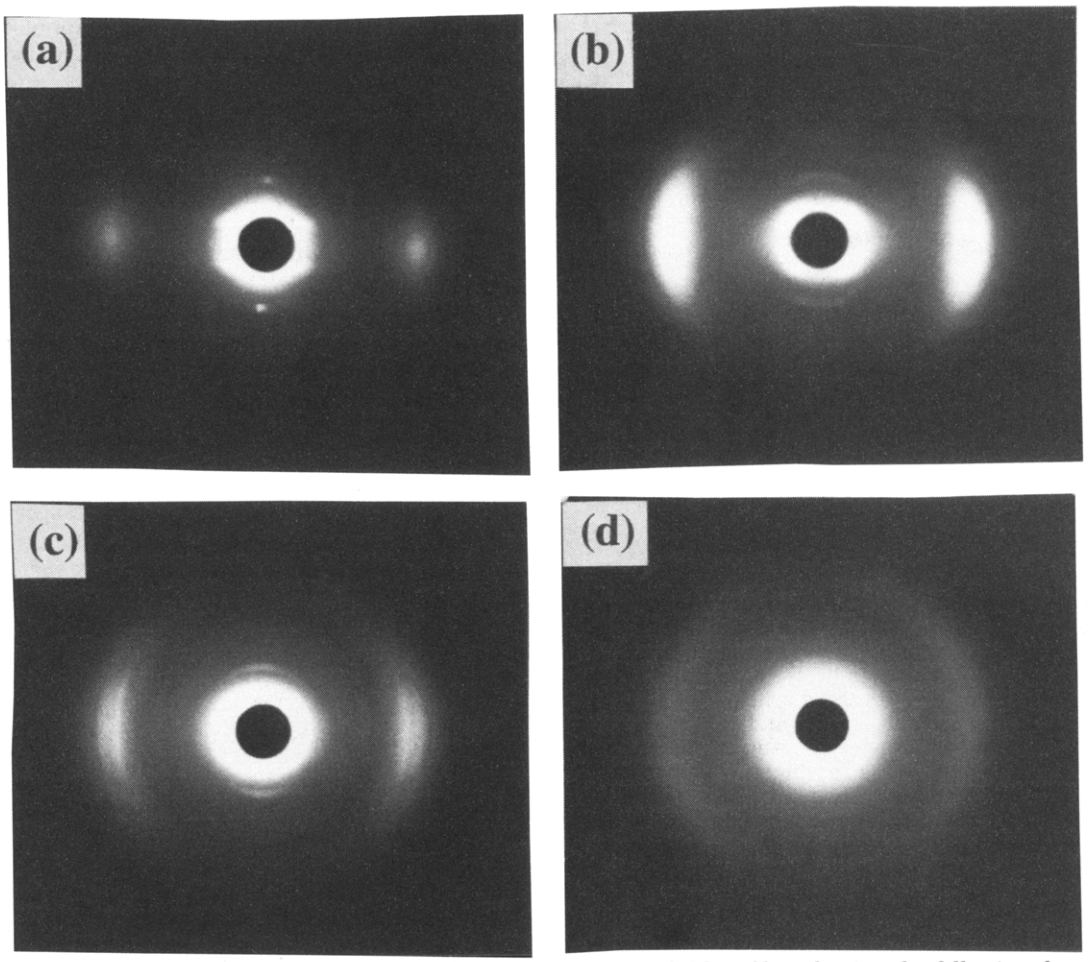

Figure 6. X-ray diffraction patterns at room temperature of melt-spun PSHQ10 fibers having the following thermal histories: (a) unannealed fiber; (b) fiber annealed at 130 °C for 1 h; (c) fiber annealed at 130 °C for 80 h; (d) fiber which was first annealed at 130 °C for 80 h and then received further thermal treatment at 165 °C for 10 min. The fiber axis is along the vertical direction.

Table 1. *d*-Spacings[a] for Unannealed Melt-Spun Fibers of PSHQ10

d (nm)
(a) meridional diffraction
0.97
0.49
(b) equatorial diffraction
0.3–0.6

[a] Four-point spots are not included in this table.

Table 2. *d*-Spacings[a] for the Melt-Spun Fibers Annealed at 130 °C for 80 h

d (nm)	comments
(a) meridional diffraction	
0.97	
0.49	
(b) equatorial diffraction	
0.60	
0.52	
0.45	strong peak
0.40	strong peak
0.36	
0.34	

[a] The inner ring is not included in this table.

worth noting in Figure 7. A comparison of panels a and b of Figure 7 indicates that the as-cast specimen without annealing has some degree of ordered structure, but its X-ray diffraction pattern is *not* as sharp as that of the as-cast specimen which was annealed at 130 °C for 80 h. This seems to suggest that the X-ray diffraction patterns observed in both the unannealed and annealed specimens have the same physical origin and that the annealed specimen has a more ordered crystallike structure. A comparison of panels c and d of Figure 7 reveals that (i) when an as-cast specimen is heated to 190 °C in the isotropic region and held there for 10 min, the X-ray diffraction pattern of the specimen is very diffuse (see Figure 7c), but when the same specimen is further annealed at 130 °C in the nematic region for 80 h, the X-ray diffraction pattern of the specimen becomes very sharp (see Figure 7d), indicating that a highly ordered crystallike structure was formed during the annealing at 130 °C for 80 h, very similar to that shown in Figure 7b. We found, however, that *d*-spacings in the two specimens are different; namely, (i) the specimen that was annealed at 130 °C for 80 h (see Figure 7b) has a *d*-spacing of 0.449 nm, and (ii) the specimen that first received thermal treatment at 190 °C for 10 min and then was annealed at 130 °C for 80 h (Figure 7d) has a *d*-spacing of 0.403 nm. It should be mentioned that both of these sharp spacings are present in the X-ray diffraction pattern of the annealed melt-spun fiber (see Figure 7c). A comparison of panels b and d of Figure 7 further reveals that the as-cast specimen annealed at 130 °C for 80 h has a larger and more uniform lateral spacing than the specimen that first received thermal treatment at 190 °C to erase previous thermal history and then was annealed at 130 °C for 80 h. The values of *d*-spacing determined for the as-cast specimens having different thermal histories are given in Tables 3 and 4.

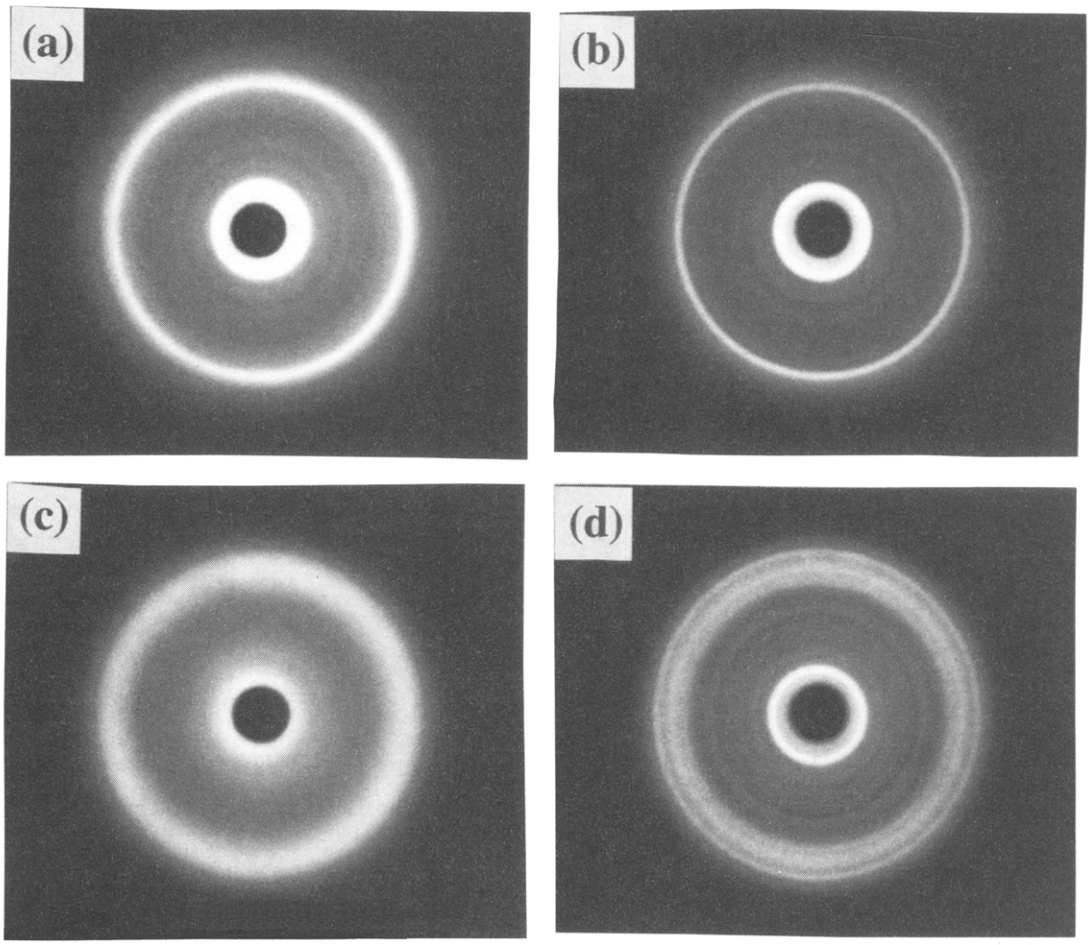

Figure 7. X-ray diffraction patterns at room temperature of as-cast PSHQ10 specimens having the following thermal histories: (a) unannealed specimen; (b) specimen annealed at 130 °C for 80 h; (c) specimen which received thermal treatment at 190 °C (in the isotropic region) for 10 min; (d) specimen which first received thermal treatment at 190 °C for 10 min and then was annealed at 130 °C for 80 h.

Table 3. *d*-Spacings for As-Cast Specimen Annealed at 130 °C for 80 h

$\sin^2\theta$	d (nm)	comments[a]
0.003 24	1.354	very strong
0.006 68	0.943	weak
0.010 78	0.743	weak
0.016 07	0.608	weak
0.019 86	0.547	weak
0.023 64	0.501	weak
0.029 03	0.453	strong
0.033 33	0.422	weak
0.037 82	0.396	weak
0.044 09	0.367	weak
0.051 45	0.340	weak
0.064 28	0.304	weak

[a] Intensity of the diffraction peak.

Table 4. *d*-Spacings for As-Cast Specimens Receiving Thermal Treatment at 190 °C for 10 min Followed by Annealing at 130 °C for 80 h

$\sin^2\theta$	d (nm)	comments[a]
0.003 24	1.354	very strong
0.006 68	0.976	weak
0.009 60	0.787	weak
0.012 70	0.684	weak
0.016 97	0.592	weak
0.018 11	0.573	weak
0.024 29	0.495	weak
0.030 15	0.444	weak
0.036 61	0.403	strong
0.041 70	0.378	weak
0.059 08	0.317	weak
0.066 03	0.300	weak

[a] The intensity of the diffraction peak.

4. Discussion

4.1. Origin of High-Temperature Melting Crystals. Above we have shown that the high-temperature melting crystal in PSHQ10 was formed during isothermal annealing. In order to investigate its origin(s), we conducted variable heating-rate DSC experiment. Below we discuss its results.

Figure 8 gives traces of variable heating rate DSC thermograms for the as-cast specimens, which were dried at 80 °C for 3 days after the majority of the solvent was evaporated at room temperature under the hood. The following observations are worth noting in Figure 8. (1) At the heating rate of 5 °C/min, three endothermic peaks appear, namely, (a) at 110.0 °C representing the melting point (i.e., T_{m2}) of low-temperature melting crystals, (b) at 140.4 °C (i.e., T_{m1}) representing the melting point of high-temperature melting crystals, and (c) at 169.8 °C representing the nematic–isotropic transition temperature (i.e., T_{NI}). (2) As the heating rate is increased from 5 to 10 and to 20 °C/min, interestingly enough, the area under the intermediate endothermic peak decreases, whereas the other endothermic peaks still persist. (3) At the heating rates of 40 and 60 °C/min, respectively, the intermediate endothermic peak does *not* appear and the low-temperature endothermic peak becomes much broader, which seems to indicate that a small amount of high-temperature melting crystals is present in the low-temperature

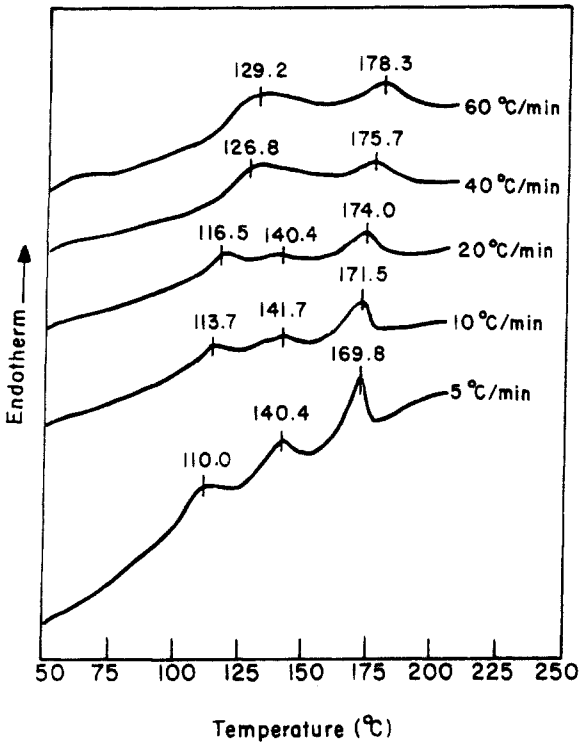

Figure 8. DSC traces for as-cast PSHQ10 specimens, which were dried at 80 °C for 3 days, at various heating rates as indicated in the figure.

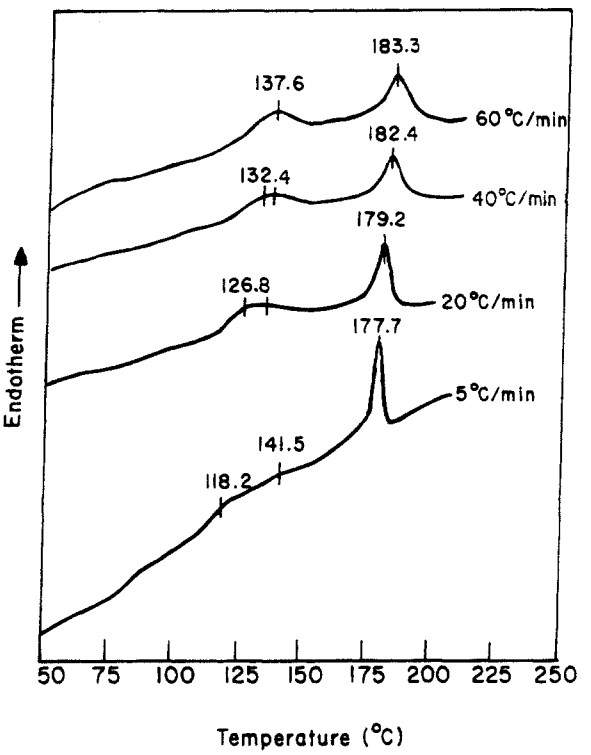

Figure 9. DSC traces for as-cast PSHQ10 specimens, which were first dried at 80 °C for 3 days and then at 120 °C for 4 h, at various heating rates as indicated in the figure.

melting crystals. The above observations lead us to conclude that (a) the intermediate endothermic peak that appeared at *low* heating rates (say, at 5 °C/min) originated from *recrystallization* taking place during the DSC run and (b) the broad low-temperature endothermic peak at high heating rates (say, at 60 °C/min) is due to the insufficient time allowed for recrystallization to take place during the DSC run. It should be pointed out that the temperature employed for drying the as-cast specimen was 80 °C, which is slightly below the glass transition temperature (~80–85 °C) of PSHQ10 and much higher than the boiling point (43 °C) of dichloromethane used as a solvent. In other words, the as-cast specimens employed in the DSC run, the results of which are summarized in Figure 8, were not annealed at all.

Figure 9 gives traces of variable heating rate DSC thermograms for the as-cast specimens which were dried further at 120 °C for 4 h after initially being dried at 80 °C for 3 days. In other words, the specimens used in the DSC runs, the results of which are given in Figure 9, had an additional thermal treatment at 120 °C for 4 h, as compared to the specimens used in the DSC runs, the results of which are given in Figure 8. The following observations are worth making in Figure 9. (1) At the heating rate of 5 °C/min, three endothermic peaks appear, namely, (a) at 118.2 °C representing T_{m2}, (b) at 141.5 °C representing T_{m1}, and (c) at 177.7 °C representing T_{NI}. Notice, however, that the sizes of the endothermic peaks for T_{m1} and T_{m2} are very small as compared to those in Figure 8 at the same heating rate. (2) As the heating rate is increased from 5 to 20 and to 40 °C/min, the distance between T_{m1} and T_{m2} becomes shorter (i.e., the two peaks appear to merge) and the peak becomes very broad. (3) At the heating rate of 60 °C/min, only two endothermic peaks are observed. We are of the opinion that most likely the endothermic peak at 137.6 °C, observed in Figure 9 at the heating rate of 60 °C/min during the DSC run, represents a combined

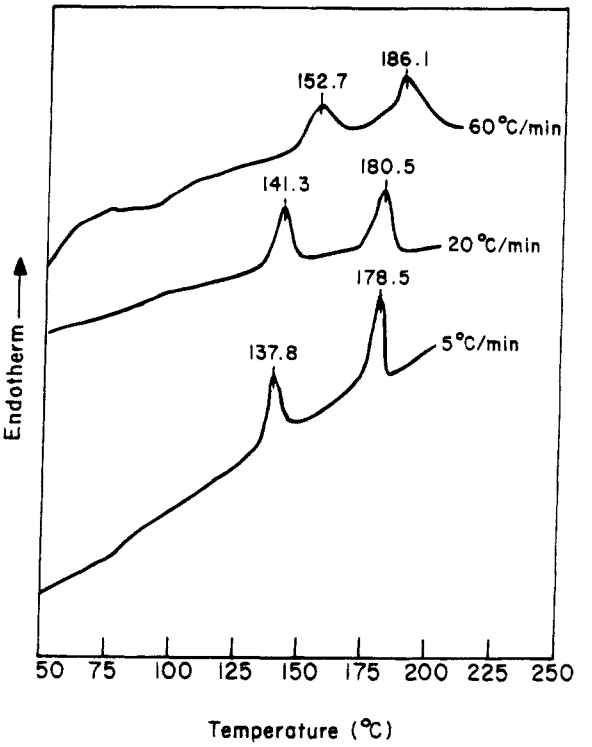

Figure 10. DSC traces for as-cast PSHQ10 specimens, which were annealed at 130 °C for 1 h after being dried first at 80 °C for 3 days and then at 120 °C for 4 h, at various heating rates as indicated in the figure.

effect of low- and high-temperature melting crystals.

A comparison of Figure 8 with Figure 9 leads us to conclude that while an as-cast specimen was further dried at 120 °C for 4 h, recrystallization appears to have taken place. Therefore the lower endothermic peak in Figure 9, which represents mainly T_{m1}, describes the melting of the high-temperature melting crystal which was formed during sample preparation by drying at 120

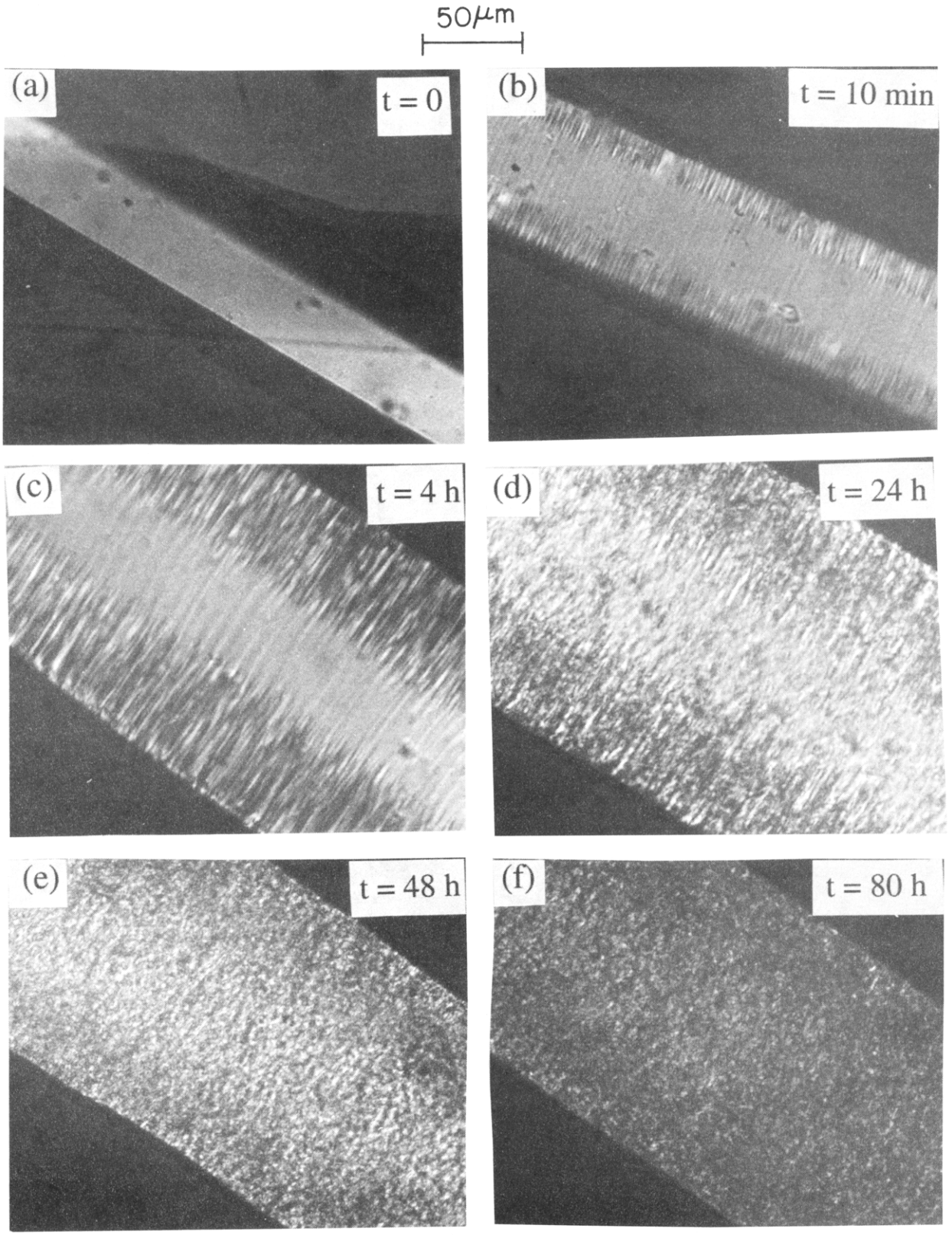

Figure 11. Cross-polarized optical micrographs describing the time evolution of the domain texture of a melt-spun PSHQ10 fiber during isothermal annealing at 130 °C for different periods, as indicated in the picture.

°C. This is different from the situation observed in Figure 8, where at the heating rate of 60 °C/min we still observe broad T_{m2}. It is worth noting in reference to Figure 9 that the intermediate endothermic peak appearing at 141.5 °C at the heating rate of 5 °C/min might have arisen (i) from the recrystallization that took place during the DSC run and/or (ii) from high-temperature melting crystals that had been formed during the drying of the specimen at 120 °C for 4 h.

Figure 10 gives traces of variable heating rate DSC thermograms for the as-cast specimens, which were annealed at 130 °C for 1 h after the specimens had been dried first at 80 °C for 3 days and then at 120 °C for 4 h; i.e., the specimens used in obtaining the DSC traces given in Figure 10 had an additional thermal treatment at 130 °C for 1 h, as compared to the specimens used for obtaining the results given in Figure 9. It can be seen in Figure 10 that, consistent with the DSC traces

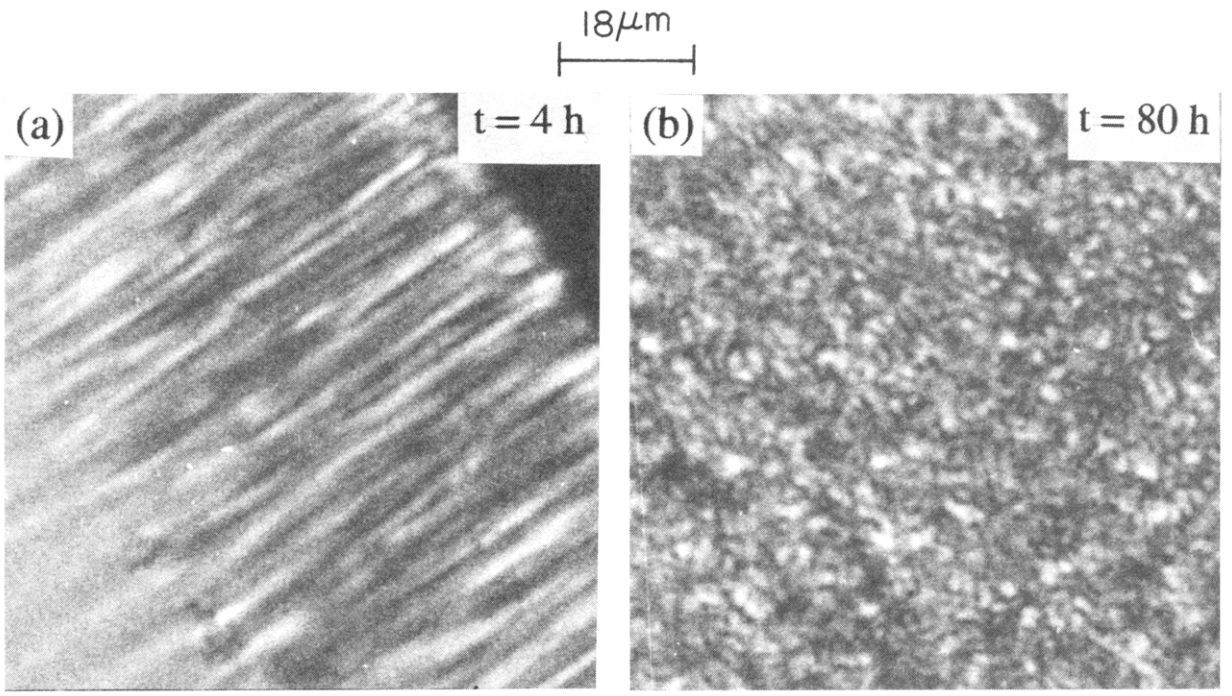

Figure 12. Enlarged micrographs of panels c and f of Figure 11, describing the domain textures of a melt-spun PSHQ10 fiber during isothermal annealing at 130 °C. The polarizer is in the horizontal direction, and the analyzer is in the vertical direction.

given in Figure 3, only two endothermic peaks appear, one representing T_{m1} and the other representing T_{NI}, regardless of the heating rates employed from 5 to 60 °C/min. It should be mentioned that the annealing temperature of 130 °C, employed in the sample preparation for the DSC runs given in Figure 10, is already higher than T_{m2}. Thus we conclude that low-temperature melting crystals melted away during the isothermal annealing at 130 °C for 1 h and recrystallization took place during the annealing, giving rise to high-temperature melting crystals. The recrystallized material has a higher melting temperature because the chains are more ordered during the isothermal annealing. As a matter of fact, the X-ray diffraction patterns support this interpretation; specifically, an as-cast specimen annealed at 130 °C for 80 h (see Figure 7b) has a much sharper diffraction pattern than the unannealed specimen (see Figure 7a). On the basis of the observations made above, we conclude that the molecular origin of the high-temperature melting crystals present in annealed PSHQ10 specimens lies in the *recrystallization* and *perfection* of the crystals during isothermal annealing.

4.2. Domain Texture of Melt-Spun PSHQ10 Fibers. In the present study, a hot-stage microscope under cross-polarized light was employed to investigate variations in domain texture in melt-spun fibers. The primary purpose of the optical microscopy study undertaken was to observe how the presence of high-temperature melting crystals, which was confirmed by DSC and WAXD, respectively, might influence the domain texture of PSHQ10. The optical microscopy study was conducted using specimens that had thermal histories identical to those employed for DSC and WAXD.

Micrographs describing the time evolution of the domain texture of a melt-spun fiber during annealing at 130 °C are given in Figure 11, in which the time (t) at which the micrographs were taken after the isothermal annealing began is given. The following observations are worth noting in Figure 11. Initially (i.e., t = 0) the melt-spun fiber shows *no* domain structure. However, the micrograph taken at t = 10 min shows a *banded structure* perpendicular to the fiber axis, and the banded structure persisted as the isothermal annealing continued for 24 h. It should be remembered from the DSC thermograms given in Figure 2 that, when annealed at 130 °C for a period of up to 24 h, melt-spun fibers exhibited two endothermic peaks, one at ~120 °C representing the melting point (T_{m2}) of low-temperature melting crystals and the other at ~180 °C representing the clearing temperature (T_{NI}). According to Kim and Han,[9] PSHQ10 has Schlieren texture at temperatures between T_{m2} and T_{NI}. Previously Kim and Han[14] demonstrated that, when sheared between two glass plates, an as-cast PSHQ10 specimen having Schlieren texture exhibited banded structure in the direction perpendicular to the shear direction. It is of interest to observe in Figure 11 that the banded structure in the melt-spun fiber disappeared when the annealing continued for 48 h and longer. It should be remembered from the DSC thermogram given in Figure 2 that high-temperature melting crystals were formed when a melt-spun fiber was annealed for 48 h and longer. We thus conclude that the disappearance of the banded structure in the melt-spun fiber upon annealing for a period of 48 h and longer, observed in Figure 11, is attributable to the formation of high-temperature melting crystals, which suppressed the appearance of the banded structure in the melt-spun fiber.

It should be mentioned that in the past a number of research groups reported the observations made of the formation of banded structures in TLCPs,[15-20] as well as in lyotropic nematics[21-24] and cholesterics.[25-29] However, very few previous studies dealt with the banded structure in a melt-spun fiber and examined how the banded structure varied with annealing conditions. In this regard, the present study appears to be the first to use the banded structure in a melt-spun fiber to investigate a phase transition in a TLCP.

In order to facilitate our discussion below, two of the micrographs given in Figure 11 were magnified and they are given in Figure 12, showing that the micrograph

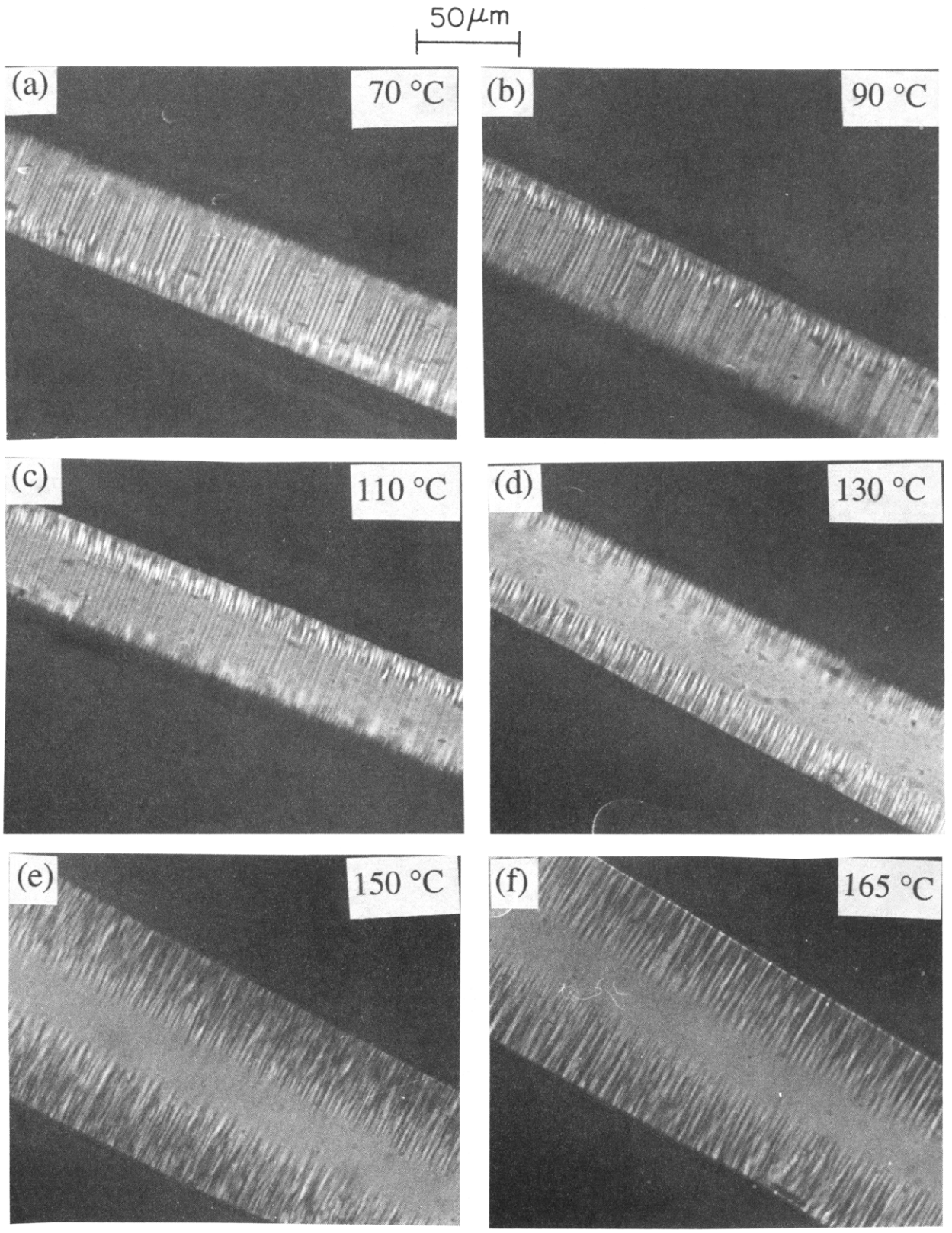

Figure 13. Cross-polarized optical micrographs describing the domain texture of a melt-spun PSHQ10 fiber, which had previously been annealed at 130 °C for 1 h, during heating from room temperature to 165 °C. The temperature was increased stepwise, and the specimen was kept at each predetermined temperature for 10 min. The polarizer is in the horizontal direction, and the analyzer is in the vertical direction.

taken 4 h after annealing began has long fibrillous texture aligned in the direction perpendicular to the fiber axis, whereas the micrograph taken 80 h after annealing began has quite different domain texture. It should be remembered that the micrograph taken 80 h after annealing began contains high-temperature melting crystals.

Figure 13 shows micrographs of a melt-spun fiber, which had been annealed at 130 °C for 1 h, during heating from 70 to 165 °C. It can be seen in Figure 13 that the melt-spun fiber exhibits banded structure over the entire range of temperatures, 70−165 °C, tested. On the basis of the DSC thermograms given in Figures 1 and 2, it can be easily surmised that when annealed at

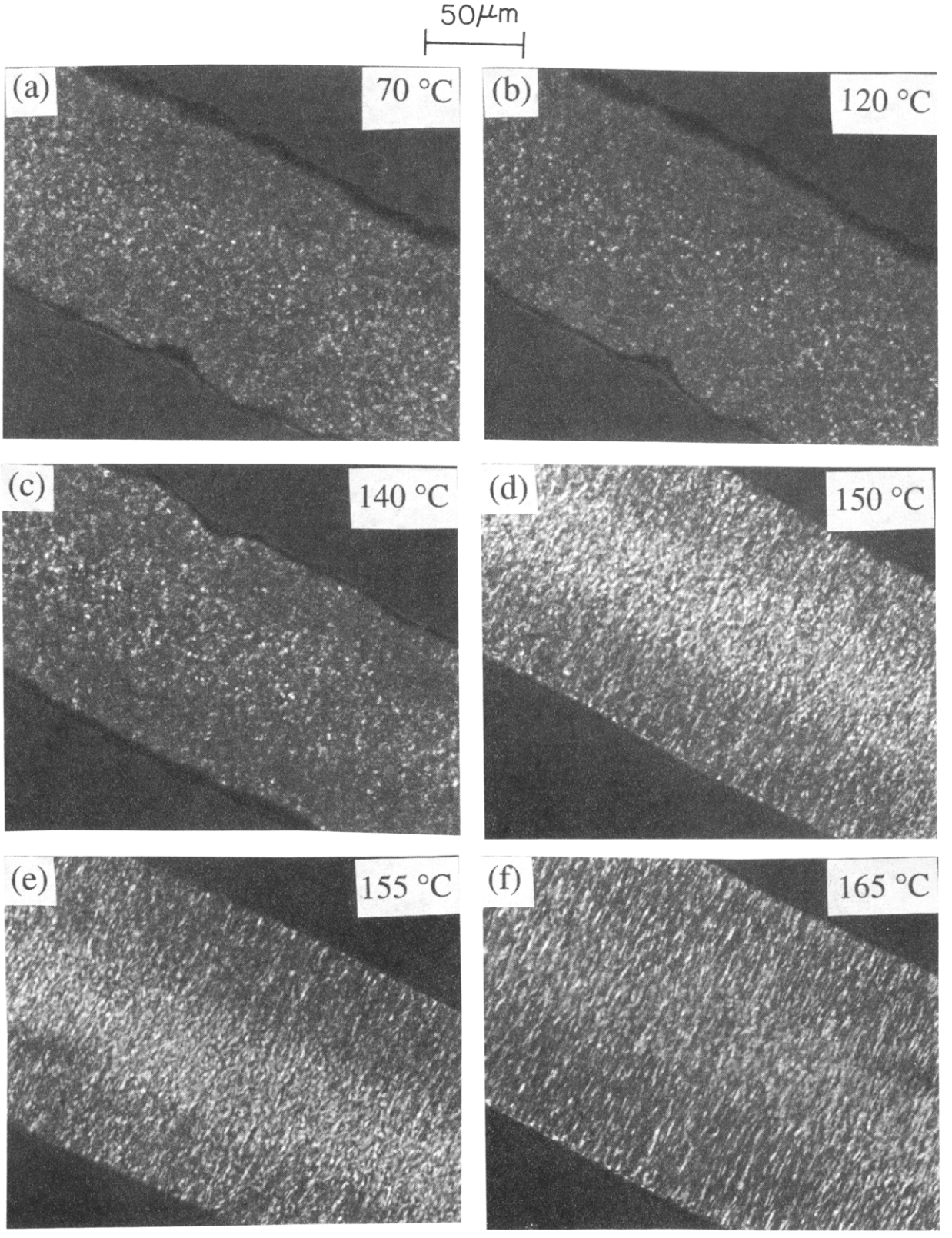

Figure 14. Cross-polarized optical micrographs describing the domain texture of a melt-spun PSHQ10 fiber, which had previously been annealed at 130 °C for 80 h, during heating from room temperature to 165 °C. The temperature was increased stepwise, and the specimen was kept at each predetermined temperature for 10 min. The polarizer is in the horizontal direction, and the analyzer is in the vertical direction.

130 °C for 1 h, a melt-spun fiber would *not* have formed high-temperature melting crystals and thus the banded structure in the melt-spun fiber was *not* suppressed at temperatures of 70−165 °C. In other words, the banded structure observed in Figure 13 is attributable to the orientation that existed in the melt-spun fiber.

Figure 14 shows micrographs taken of a melt-spun fiber, which had been annealed at 130 °C for 80 h, during heating from 70 to 165 °C. The following observations are worth noting in Figure 14. As the melt-spun fiber was heated to 140 °C, it exhibited a domain texture which resembles some kind of crystalline structure. As the melt-spun fiber was heated to 150 °C, the banded structure began to appear and it

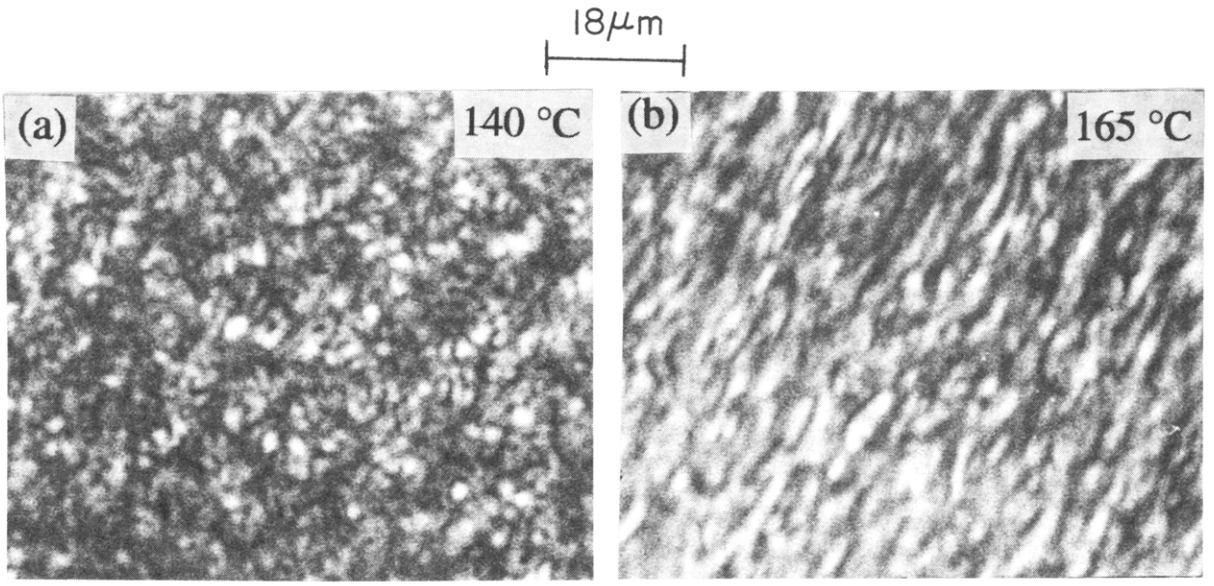

Figure 15. Enlarged micrographs of panels c and f of Figure 14, describing the domain textures of a melt-spun PSHQ10 fiber during heating from room temperature to 165 °C. The polarizer is in the horizontal direction, and the analyzer is in the vertical direction.

became more distinct as the temperature was increased further to 155 and to 165 °C. It should be remembered from the DSC thermograms given in Figure 2 that a melt-spun fiber, which was annealed at 130 °C for 80 h, has high-temperature melting crystals which melt away at ~150 °C. This temperature corresponds to the one at which banded structure in the melt-spun fiber begins to appear in Figure 14. In order to facilitate our discussion here, two of the micrographs given in Figure 14 were magnified and they are given in Figure 15. A comparison of Figure 12b with Figure 15a reveals that the domain textures in the presence of high-temperature melting crystals are virtually identical. It is of interest to note that (a) the fiber orientation was distorted by the formation of high-temperature melting crystals, and (b) after the high-temperature melting crystals melted away, the banded structure which was formed in the oriented fiber still exists on the fiber (compare Figures 11c and 14f). This seems to suggest that the high-temperature melting crystals have (a) an extended chain conformation, indicative of crystal perfection by rigid macromolecules, and (b) regularity in lateral spacings in the crystal structure, evidence of which can be seen in the X-ray diffraction pattern given in Figure 6c.

5. Concluding Remarks

In this paper we have shown that PSHQ10, which is a main-chain thermotropic homopolyester having flexible spacers and bulky side groups, exhibits dual endothermic peaks on DSC thermograms, one at a temperature (T_{m2}) of ~120 °C and the other at a temperature (T_{m1}) of ~150 °C, below its clearing temperature T_{NI}. We have identified T_{m2} as the melting point of low-temperature melting crystals and T_{m1} as the melting point of high-temperature melting crystals. The appearance of T_{m1} on DSC thermograms is found to depend on the thermal history of the specimen. Specifically, in an as-cast specimen T_{m1} appears soon after annealing began in the nematic region, whereas in a melt-spun fiber it appears ~40 h after annealing began in the nematic region. However, when an as-cast specimen was first heated to the isotropic region and then cooled to the nematic region, we found that T_{m1} appears ~40 h after annealing began in the nematic region. That is, the formation of high-temperature melting crystals in PSHQ10 is delayed ~40 h when it was first heated to a temperature in the *isotropic* region. Such an observation is very important to establishing reproducible initial conditions for rheological measurements and thus reproducible rheological data for PSHQ10[30-33] and perhaps for other types of TLCPs.

We have determined via WAXD the structure of high-temperature melting crystals present in annealed PSHQ10 specimen. Specifically, (i) Figure 6a shows the X-ray diffraction pattern for an *unannealed* melt-spun fiber which, according to Figure 1, has only low-temperature melting crystals, and (ii) Figure 7b shows the X-ray diffraction patterns for an annealed as-cast specimen which, according to Figure 2, has *no* lower temperature endothermic peak when annealed at 130 °C for 48 h or longer. Thus, a detailed study via lower angle X-ray diffraction (preferably small-angle X-ray scattering) would be needed in order to examine the X-ray diffraction patterns inside the inner ring of Figures 6a and 7b, respectively.

When taking a close look at the X-ray diffraction patterns, given in Figure 6c, of the melt-spun fibers which were annealed at 130 °C for 80 h, we notice a ring, characteristic of small-angle diffraction patterns, which is attributable to the chain rotation caused by the twisted textures that were observed under a cross-polarized optical microscope. According to the DSC thermograms given in Figure 2, the melt-spun fiber after being annealed at 130 °C for 80 h exhibits only an intermediate endothermic peak, but not a lower temperature endothermic peak. It should be noted that the same fiber, when annealed for a period of less than 24 h, exhibits only the lower temperature endothermic peak. In view of the fact that the area under the lower temperature endothermic peak is very small as compared to the area under the intermediate endothermic peak, it is fair to state that when a melt-spun fiber is annealed to 130 °C for 80 h, the lower temperature endothermic peak is not seen because it was greatly suppressed by the presence of high-temperature melting crystals. It should be remembered that the larger the value of T_{m1}, the smaller the area under the T_{m2} peak. This suggests to us that the two melting peaks have a

common crystal packing structure but slightly different lateral packing spacings and that high-temperature melting crystals have more perfectly ordered lateral spacing than low-temperature melting crystals.

Also, using optical microscopy under cross-polarized light, we investigated the effect of thermal history on the domain texture of PSHQ10, which had been subjected to the same thermal history as the specimens employed for WAXD. The findings from WAXD and optical microscopy suport the DSC results. From the results obtained in this study, we conclude that the molecular origin of the high-temperature melting crystals present in annealed PSHQ10 specimens lies in the *recrystallization* and *perfection* of the crystals during isothermal annealing.

Before closing, it should be mentioned that the literature[23,24,29,34,35] indicates that the formation of banded structure in a liquid-crystalline polymer is associated with a transient phenomenon; namely, banded structure appear after cessation of flow (in shear or elongation). On the other hand, in the present study we observed banded structure in a melt-spun PSHQ10 fiber, and the banded structure persisted during isothermal annealing for over 24 h, but disappeared only after the isothermal annealing continued for a period of over 48 h. We attribute the disappearance of the banded structure to the formation of high-temperature melting crystals, which began only after the annealing continued for ~48 h. It appears that the formation of banded structure in the melt-spun PSHQ10 fiber, observed in the present study, is not related to a transient phenomenon. This is a subject for future investigation.

Acknowledgment. We acknowledge with deep gratitude Professor Benjamin Chu and Dr. Y. Li at the Department of Chemistry, State University of New York at Stony Brook, who have kindly undertaken measurements of wide-angle X-ray diffraction of our samples at elevated temperatures, the results of which are reproduced in Figure 5.

References and Notes

(1) Krigbaum, W. R.; Salaris, F. *J. Polym. Sci., Polym. Phys. Ed.* **1978**, *16*, 883.
(2) Griffin, A.; Havens, S. J. *J. Polym. Sci., Polym. Phys. Ed.* **1981**, *19*, 951.
(3) Butzbach, G. D.; Wendorff, J. H.; Zimmermann, H. J. *Polymer* **1986**, *27*, 1337.
(4) Cheng, S. Z. D. *Macromolecules* **1988**, *21*, 2475.
(5) Cheng, S. Z. D.; Janimak, J. J.; Zhang, A.; Zhou, Z. *Macromolecules* **1989**, *22*, 4240.
(6) Cheng, S. Z. D.; Zhang, A.; Johnson, R. L.; Wu, Z.; Wu, H. H. *Macromolecules* **1990**, *23*, 1196.
(7) Nam, J.; Fukai, T.; Kyu, T. *Macromolecules* **1991**, *24*, 6250.
(8) Lin, Y. G.; Winter, H. H. *Macromolecules* **1988**, *21*, 2439.
(9) Kim, S. S.; Han, C. D. *Macromolecules* **1993**, *26*, 3176.
(10) Bhowmik, P. K.; Garay, P. O.; Lenz, R. W. *Makromol. Chem.* **1991**, *192*, 415.
(11) Sweet, G. E.; Bell, J. P. *J. Polym. Sci. A-2* **1973**, *10*, 1273.
(12) Furukawa, A.; Lenz, R. W. *Macromol. Chem., Macromol. Symp.* **1986**, *2*, 3.
(13) Kim, S. S.; Han, C. D. *Polymer* **1994**, *35*, 93.
(14) Kim, S. S.; Han, C. D. *J. Polym. Sci., Polym. Phys. Ed.* **1994**, *32*, 371.
(15) Donald, A. M.; Viney, C.; Windle, A. H. *Polymer* **1983**, *24*, 155.
(16) Viney, C.; Donald, A. M.; Windle, A. H. *J. Mater. Sci.* **1983**, *18*, 1136.
(17) Donald, A. M.; Windle, A. H. *J. Mater. Sci.* **1983**, *18*, 1143.
(18) Zachariades, A. E.; Navard, P.; Logan, J. P. *Mol. Cryst. Liq. Cryst.* **1984**, *110*, 93.
(19) Navard, P.; Zachariades, A. E. *J. Polym. Sci., Polym. Phys. Ed.* **1987**, *25*, 1089.
(20) Takeuchi, Y.; Shuto, Y.; Yamamoto, F. *Polymer* **1988**, *29*, 605.
(21) Fincher, C. R. *Macromolecules* **1986**, *19*, 2431.
(22) Viney, C.; Windle, A. H. *Philos. Mag.* **1987**, *A55*, 463.
(23) Marsano, E.; Carpaneto, L.; Ciferri, A.; Wu, Y. *Liq. Cryst.* **1988**, *3*, 1561.
(24) Chapoy, L. L.; Marcher, R.; Rasmussen, K. H. *Liq. Cryst.* **1988**, *3*, 1161.
(25) Kiss, G.; Porter, R. S. *Mol. Cryst. Liq. Cryst.* **1980**, *60*, 267.
(26) Nishio, Y.; Yamane, Y.; Takahashi, T. *J. Polym. Sci., Polym. Phys. Ed.* **1985**, *23*, 1053.
(27) Navard, P. *J. Polym. Sci., Part B: Polym. Phys.* **1986**, *24*, 435.
(28) Fried, F.; Sixou, P. *Mol. Cryst. Liq. Cryst.* **1988**, *158B*, 163.
(29) B. Ernst E.; Navard, P. *Macromolecules* **1989**, *22*, 1419.
(30) Kim, S. S.; Han, C. D. *Macromolecules* **1993**, *26*, 6633.
(31) Kim, S. S.; Han, C. D. *J. Rheol.* **1993**, *37*, 847.
(32) Han, C. D.; Kim, S. S. *J. Rheol.* **1994**, *38*, 13.
(33) Han, C. D.; Kim, S. S. *J. Rheol.* **1994**, *38*, 31.
(34) Marsano, E.; Carpeneto, L.; Ciferri, A. *Mol. Cryst. Liq. Cryst.* **1988**, *158*, 267.
(35) Gleeson, J. T.; Larson, R. G.; Mead, D. W.; Kiss, G.; Cladis, P. E. *Liq. Cryst.* **1992**, *11*, 341.